DMD Fast Forward. Published on April 21, 2011 as doi:10.1124/dmd.110.037812

DMD # 37812

Cannabinoid CB1 receptor antagonists modulate transport activity of multidrug resistance-associated proteins MRP1, MRP2, MRP3, and MRP4

Hanneke G.M. Wittgen, Jeroen J.M.W. van den Heuvel, Petra H. H. van den Broek, Heike Dinter-Heidorn, Jan B. Koenderink, Frans G.M. Russel

Department of Pharmacology and Toxicology, Radboud University Nijmegen Medical Centre, Nijmegen Centre for Molecular Life Sciences, the Netherlands (H.G.M.W, J.J.M.W.v.d.H, P.H.H.v.d.B, J.B.K., F.G.M.R.); Abbott Products GmbH, Hannover, Germany (H.D.H.)

DMD Fast Forward. Published on April 21, 2011 as DOI: 10.1124/dmd.110.037812
This article has not been copyedited and formatted. The final version may differ from this version.

Running title: CB1 receptor antagonists interact with MRP1-4

Address correspondence to: Prof. F.G.M. Russel, PhD, Department of Pharmacology and Toxicology (149), Radboud University Nijmegen Medical Centre, Nijmegen Centre for Molecular Life Sciences, P. O. Box 9101, 6500 HB Nijmegen, the Netherlands. Tel.: +31 24 3616892; Fax: +31 24 3614214; E-mail: F.Russel@pharmtox.umcn.nl

Text pages: 22

Tables: 2

Figures: 5

References: 41

Words in abstract: 236

Words in introduction: 674

Words in discussion: 1283

Abbreviations: CB, cannabinoid; MRP, multidrug resistance-associated protein; $E_2$17βG, estradiol-17-β-D-glucuronide; HEK293, human embryonic kidney 293 cells; E-64, *N*-(*trans*-epoxysuccinyl)-L-leucine 4-guanidinobutylamide; DMEM, Dulbecco Eagle's modified medium; eYFP, enhanced yellow fluorescent protein

Abstract

Cannabinoid type 1 (CB1) receptor antagonists have been developed for the treatment of obesity, but a major disadvantage is that they cause unwanted psychiatric effects. Selective targeting of peripheral CB1 receptors might be an option to circumvent these side effects. Multidrug resistance-associated proteins (MRPs) can influence the pharmacokinetics of drugs and thereby affect their disposition in the body. In this study, we investigated the interaction of the prototypic CB1 receptor antagonist rimonabant and a series of 3,4-diarylpyrazoline CB1 receptor antagonists with MRP1, MRP2, MRP3, and MRP4 *in vitro*. Their effect on ATP-dependent transport of estradiol 17-β-D-glucuronide was measured in inside-out membrane vesicles isolated from transporter-overexpressing HEK293 cells. Rimonabant inhibited MRP1 transport activity more potently than MRP4 (K_i of 1.4 μM and 4 μM, respectively), whereas the 3,4-diarylpyrazolines were stronger inhibitors of MRP4 than MRP1-mediated transport. A number of CB1 receptor antagonists, including rimonabant, stimulated MRP2 and MRP3 transport activity at low, but inhibited $E_2$17βG transport at high substrate concentrations. The interaction of 3,4-diarylpyrazolines and rimonabant with MRP1-4 indicate their potential for drug-drug interactions. Preliminary *in vivo* data suggested that for some 3,4-diarylpyrazolines the relatively lower brain efficacy may be related to their inhibitory potency against MRP4 activity. Furthermore, this study shows that the modulatory effects of the 3,4-diarylpyrazolines were influenced by their chemical properties, and that small variations in structure can determine the affinity of these compounds for efflux transporters and thereby affect their pharmacokinetic behavior.

DMD Fast Forward. Published on April 21, 2011 as DOI: 10.1124/dmd.110.037812
This article has not been copyedited and formatted. The final version may differ from this version.

Introduction

The cannabinoid type 1 (CB1) receptor is involved in regulation of feeding behavior, metabolism, and energy balance (Di Marzo, 2008). Studies in rodents have shown that antagonism of this receptor leads to reduced food intake and weight reduction (Boyd and Fremming, 2005). Several CB1 receptor antagonists were developed for the treatment of obesity, and clinical studies showed a reduction in appetite, weight loss, and improved metabolic risk factors (Boyd and Fremming, 2005;Bifulco et al., 2009). Rimonabant was the first and only selective CB1 receptor antagonist approved for therapeutic use. However, the drug was withdrawn from the market within two years of its introduction, because psychiatric adverse effects, in particular depression, were revealed in additional clinical studies (Jones, 2008;Nissen et al., 2008).

The CB1 receptor is expressed in brain and peripheral tissues such as adipose, skeletal muscle, liver, gut, and pancreas (Di Marzo, 2008). In the brain, activation of the endocannabinoid system appears to be involved in coping with stress and anxiety. Therefore, the psychiatric side effects seen for CB1 receptor antagonists could be due to inhibition of the endocannabinoid system (Bifulco et al., 2009). It is believed that the positive effect of antagonists on metabolic factors could also be mediated via peripheral CB1 receptors (Di Marzo, 2008). Indeed, a recent study with a peripheral CB1 receptor antagonist in obese mice showed that this antagonist could improve the cardiometabolic risk in these mice without inhibition of the central CB1 receptor (Tam et al., 2010). Therefore, peripheral CB1 receptor antagonists might have therapeutic potential for improving metabolic risk in obese patients, without causing psychiatric side effects.

Multidrug resistance-associated proteins (MRPs) are efflux transporters that can influence drug disposition by transporting a wide variety of substrates out of the cell (Zhou et al., 2008), preventing drugs from entering specific tissues or organs (*e.g.* intestine and brain), or increasing elimination of compounds, *e.g.* via liver and kidney (Yu et al., 2007). MRP1, MRP2, MRP3, and MRP4 belong to the ATP-binding cassette (ABC) transporter subfamily C, and have overlapping substrate specificities (Kruh and Belinsky, 2003). MRP1 is present in many tissues, with highest protein expression in lung, adrenal gland, heart, and skeletal muscle, and lower amounts in brain, choroid plexus, spleen, kidney, intestine, testes, placenta, and liver (Flens et al., 1996;Rao et al.,

1999;Leslie et al., 2005;Nies et al., 2004). It is expressed basolaterally in most tissues, but it has an apical localization in brain capillary endothelial cells (Leslie et al., 2005;Nies et al., 2004). MRP2 is highly expressed in liver, and lower expression levels can be found in the apical membranes of kidney tubules, gastrointestinal tract, gall bladder, placenta, and bronchi (Nies and Keppler, 2007;van Aubel et al., 2000). MRP3 is expressed in kidney, colon, small intestine, liver, and gall bladder, where it is found mostly in basolateral membranes (Scheffer et al., 2002). MRP4 is widely distributed in tissues and blood cells and has a dual membrane localization, which is basolateral in prostate tubuloacinar cells, hepatocytes, and choroid plexus, and apical in kidney proximal tubule cells, and brain capillary endothelium (Russel et al., 2008;Nies et al., 2004). The expression of MRP1-4 at locations which are involved in drug disposition and penetration suggests that they influence drug concentrations in plasma and different organs, and, because of their presence in the blood-brain-barrier (BBB) and choroid plexus, MRP4 and MRP1 might play a role in restricting CB1 receptor antagonists from the brain.

Interaction of a drug with efflux transporters could not only influence its own pharmacokinetics, but it can also change the disposition of other compounds that are substrates for the same transporter. Studies describing the interaction of CB1 receptor antagonists with MRP1-4 may not only give information on the pharmacokinetics of these antagonists, but also on possible drug-drug interactions. Here, we investigated the *in vitro* effect of a series of 3,4-diarylpyrazoline CB1 receptor antagonists (Fig. 1) (Lange et al., 2005) and the prototypic CB1 receptor antagonist rimonabant on MRP1-4 transport activity. In addition, for some 3,4-diarylpyrazolines, we related their transporter interaction to preliminary *in vivo* pharmacodynamic effects measured in rats.

DMD Fast Forward. Published on April 21, 2011 as DOI: 10.1124/dmd.110.037812
This article has not been copyedited and formatted. The final version may differ from this version.

Materials and methods

Materials. [6,7-^{3}H(N)]-estradiol 17-β-D-glucuronide (41.8 Ci/mmol) was purchased from Perkin Elmer (Groningen, the Netherlands). Bac-to-Bac and Gateway system, DMEM + Glutamax-I culture medium, and fetal calf serum were purchased from Invitrogen (Breda, The Netherlands). Triple flasks (500 cm^2) were purchased from Sanbio BV Biological Products (Uden, The Netherlands). Estradiol 17-β-D-glucuronide ($E_2$17βG), adenosine 5'-triphosphate magnesium salt (from bacterial source) and adenosine 5'-monophosphate monohydrate (from yeast) were purchased from Sigma-Aldrich (Zwijndrecht, the Netherlands). Protein concentrations were determined with a Bio-Rad protein assay kit from Bio-Rad Laboratories (Veenendaal, The Netherlands). Monoclonal mouse-anti-human MRP3 antibody M3II-21 was purchased from Abcam (Cambridge, UK). Monoclonal mouse-anti-human MRP1 (QCRL-1) was kindly provided by Dr. S.P.C. Cole (Queen's University Cancer Research Institute, Kingston, Canada). 3,4-Diarylpyrazoline CB1 receptor antagonists (Lange et al., 2005) and rimonabant were kindly provided by Solvay Pharmaceuticals (Hannover, Germany - Solvay Pharmaceuticals is now Abbott).

Generation of baculovirus. Full-length human MRP1, MRP2, and MRP3 were cloned separately into the Gateway pDONR221vector. The sequence of MRP1 was equal to GenBank accession number NM_004996 except for three silent mutations at bp 1684, 1704, and 4002, which are known polymorphisms (Conrad et al., 2001). The sequence of MRP2 was equal to NM_000392 except for three silent mutations at bp 264, 1167, and 3972, of which C3972T is a known polymorphism (Ito et al., 2001), and the sequence of MRP3 was equal to NM_003786. Consequently, constructs were also cloned into a VSV-G improved pFastBacDual vector for mammalian cell transduction using the Gateway system (El-Sheikh et al., 2007). Full-length human MRP4 and enhanced yellow fluorescent protein (eYFP), which was used as a negative control, were already cloned before (El-Sheikh et al., 2007). Baculoviruses were produced as described in the Bac-to-Bac manual (Invitrogen).

Cell culture and transduction of HEK293 cells. HEK293 cells were grown in DMEM-Glutamax-I supplemented with 10% fetal calf serum at 37°C under 5% CO_2-humidified air. HEK293 cells were

DMD Fast Forward. Published on April 21, 2011 as DOI: 10.1124/dmd.110.037812
This article has not been copyedited and formatted. The final version may differ from this version.

cultured in 500 cm^2 triple flasks until 40% confluent, after which culture medium was removed and 25 ml medium and 10 ml eYFP, MRP1, MRP2, MRP3, or MRP4 baculovirus was added. Cells were incubated for 15 min at 37°C, after which a further 40 ml medium was added. 5 mM sodium butyrate was added 24 hours after transduction. Three days after transduction, cells were harvested by centrifugation at 5000*g* for 5 minutes.

Isolation of membrane vesicles and protein analysis. Membranes were isolated according to a previously described method with slight modifications (El-Sheikh et al., 2008). In brief, harvested cell pellets were resuspended in ice-cold homogenization buffer (0.5 mM sodium phosphate and 0.1 mM EDTA) supplemented with protease inhibitors (100 µM phenylmethylsulfonyl fluoride, 5 µg/ml aprotinin, 5 µg/ml leupeptin, 1 µg/ml pepstatin, and 1 µM E-64) and shaken at 4°C for 30 minutes. Lysed cells were centrifuged at 100,000*g* for 30 min at 4°C, and the pellets were homogenized in ice-cold TS buffer (10 mM Tris-HEPES, and 250 mM sucrose, pH 7.4) supplemented with protease inhibitors described above, using a tight-fitting Dounce homogenizer for 25 strokes. After centrifugation at 1000*g* for 20 minutes at 4°C, the supernatant was centrifuged at 100,000*g* for 60 min at 4°C. The resulting pellet was resuspended in TS buffer without protease inhibitors and passed through a 27-gauge needle 25 times. Protein concentration was determined by Bio-Rad protein assay kit. Crude membrane vesicles were dispensed in aliquots, frozen in liquid nitrogen, and stored at -80°C until further use.

Western blotting. Membrane vesicle preparations were solubilized in SDS-polyacrylamide gel electrophoresis sample buffer and separated on SDS gel, containing 7.5% acrylamide, according to Laemmli (1970). Subsequently, they were blotted on nitrocellulose membrane using the iBlot dry blotting system (Invitrogen). Monoclonal mouse-anti-human MRP1 (QCRL-1, 1:700) and MRP3 (M3II-21, 1:200) antibodies and affinity-purified, polyclonal rabbit-anti-human MRP2 (pAb hM2-p2, 1:500) and MRP4 (pAb hM4-p4, 1:1000) (Smeets et al., 2004;van Aubel et al., 2002) were used to detect transporters. The secondary antibodies used in 1:10,000 dilution were fluorescent goat-anti-mouse IRdye800 (Rockland Immunochemicals, Gilbertsville, USA) and goat-anti-rabbit Alexa Fluor

DMD Fast Forward. Published on April 21, 2011 as DOI: 10.1124/dmd.110.037812
This article has not been copyedited and formatted. The final version may differ from this version.

680 (Invitrogen). Signals were visualized using the Odyssey imaging system (Li-Cor Biosciences, Lincoln, NE).

Vesicular transport assays. Uptake of [^{3}H]$E_2$17βG into membrane vesicles was performed using a rapid filtration technique (van Aubel et al., 1999). 30 µl reaction mix consisted of TS buffer, 4 mM ATP, 10 mM $MgCl_2$, $E_2$17βG and 7.5 µg of membrane vesicles. 0.1 (MRP1), 0.15 (MRP2, MRP4), and 0.2 µCi (MRP3) [^{3}H]$E_2$17βG was used, supplemented with unlabeled $E_2$17βG to concentrations indicated in legends. The reaction was started when the mixture was incubated at 37°C and then stopped by placing samples on ice and adding 150 µl of ice-cold TS buffer. A Multiscreen$_{HTS}$ HV, 0.45 µM, PVDF 96-well filter plate was pre-washed with TS buffer and diluted samples were filtered through this filter plate using a Multiscreen$_{HTS}$-Vacuum Manifold filtration device (Millipore, Etten-Leur, The Netherlands). The filters were washed twice with TS-buffer and were then separated from the plate. After addition of 2 ml of scintillation fluid to each filter and subsequent liquid scintillation counting, uptake of [^{3}H]$E_2$17βG into membrane vesicles was determined by measuring radioactivity associated with the filters. In control experiments, ATP was substituted with AMP. Net ATP-dependent transport was calculated by subtracting values measured in the presence of AMP from those measured in the presence of ATP. Time-dependent transport was found to be linear up to 5 minutes for MRP1, MRP2, and MRP4, and up to 3 minutes for MRP3 (results not shown).

Vesicular interaction assays. To evaluate the inhibitory effects of 3,4-diarylpyrazolines and rimonabant on [^{3}H]$E_2$17βG uptake in MRP1, 2, 3, and 4 inside-out membrane vesicles, the abovementioned transport assay was performed in the absence or presence of 10 and 100 µM of CB1 receptor antagonists. The concentration-dependent effect of 1-100 µM of compounds 13, 15, and rimonabant was measured at three different $E_2$17βG concentrations: 0.16, 1, and 5 µM for MRP1; 2, 20, and 200 µM for MRP2; 0.08, 1, and 5 µM for MRP3; and 0.1, 0.3, and 1 µM for MRP4. ATP-dependent transport was calculated.

DMD Fast Forward. Published on April 21, 2011 as DOI: 10.1124/dmd.110.037812
This article has not been copyedited and formatted. The final version may differ from this version.

Determination of actual concentrations of 3,4-diarylpyrazolines and rimonabant with LC-MS/MS. The actual amount of CB1 receptor antagonists dissolved under vesicular transport assay conditions was measured. eYFP vesicles (7.5 µg) were added in each well to mimic the vesicle environment. The reaction mixture without [^{3}H]$E_2$17βG was added on ice and only the AMP-condition was measured. The 96-wells plate was mixed and the total reaction mixture from one well was transferred to an eppendorf tube at room temperature. Sample was spinned down at maximum speed (16,000-20,000*g*) for 5 minutes at room temperature and 10 µl of supernatant was reconstituted in 50% acetonitrile/water and 0.1% trifluoroacetic acid (TFA) prior to LC-MS/MS analysis. Determination of actual concentration was carried out using an Accela U-HPLC (Thermo Fisher Scientific) coupled to a TSQ Vantage (Thermo Fisher Scientific) triple quadropole mass spectrometer. The CB1 receptor antagonists were separated on a Zorbax Eclipse Plus column (50 x 2.1 mm, 1.8 µm particle size; Agilent). The elution gradient was: 0 min 50% B, 5 min 90% B, 6 min 50% B. Solvent A consisted of 0.1% TFA in ultrapure water and solvent B consisted of 0.1% TFA in acetonitrile. The column temperature was set at 40°C and the flow rate was 200 µl/min. The effluent from the HPLC was passed directly into the electrospray ion source. Positive electrospray ionization was achieved using a nitrogen sheath gas with ionization voltage at 4 kV. The capillary temperature was set at 350°C. Detection of each analyte was based on isolation of the protonated molecular ion, $[M+H]^+$, and subsequent MS/MS fragmentations and a selected reaction monitoring (SRM) were carried out. The conditions per compound are summarized in Table 1. CB1 receptor antagonist 4 or 16 was used as internal standard and the response ratio of test compound to internal standard was used to determine the concentration. Actual assay concentration of compound was measured in duplicate in at least three independent experiments.

***In vivo* pharmacodynamic effect of 3,4-diarylpyrazolines on CP55,940 induced hypotension in rat.** The ED_{50} of 3,4-diarylpyrazolines for attenuation of CP55,940 induced hypotension in male, normotensive, anaesthetized Wistar rats was determined according to a previously described method using different intravenous doses (n=2 per dose) of CB1 receptor antagonists 10 minutes before CP55,940 (0.1 mg/kg i.v.) administration (Lange et al., 2004). Hypotension was achieved within 1

DMD Fast Forward. Published on April 21, 2011 as DOI: 10.1124/dmd.110.037812
This article has not been copyedited and formatted. The final version may differ from this version.

minute after administration of the CB1 receptor agonist CP55,940, and the lowest blood pressure was the measure of the hypotensive effect. ED_{50} was calculated on the linear part of the percentage dose response curve and is the dose of antagonist that inhibited the hypotensive effect of CP55,940 by 50%. Experiments were approved by the local ethical committee on animal experimentation at Solvay Pharmaceuticals in Weesp.

Kinetic Analysis. All data were expressed as means ± S.E.M. Curve fitting of the resulting concentration-dependent transport curves and determination of IC_{50} values for the CB1 receptor antagonists was performed by non-linear regression analysis using GraphPad Prism software, version 5.02 (GraphPad Software Inc., San Diego, CA). The following equation was fitted to the data: *y* = bottom + (top-bottom)/(1 + 10^((logIC_{50} - *x*)*hill slope)), in which *x* is log inhibitor concentration and *y* is expressed as uptake versus control (%). Michaelis-Menten fit was used for MRP1, MRP3, and MRP4 $E_2$17βG curves, allosteric sigmoidal fit for MRP2. Log (inhibitor or stimulator) vs response with variable slope was used to plot the inhibition and stimulation curves with 13, 15, or rimonabant. Results of the inhibition assay for interaction of MRP1/4 with 13 and rimonabant were analyzed using Dixon's method combined with linear regression analysis to estimate the inhibitory constant (K_i). Statistical differences were determined using a one-way analysis of variance with Dunnett's multiple comparison test in GraphPad Prism. Differences were considered to be significant at $p < 0.05$.

DMD Fast Forward. Published on April 21, 2011 as DOI: 10.1124/dmd.110.037812
This article has not been copyedited and formatted. The final version may differ from this version.

Results

Expression of MRP1, MRP2, MRP3, and MRP4 in isolated membrane vesicles

Immunoblot analysis performed on membrane vesicles from HEK293 cells overexpressing MRP1, MRP2, MRP3, and MRP4 demonstrated that all four transporters were successfully expressed (data not shown). MRP1 seemed to be less glycosylated as indicated by the band at ~160 kD, but this had no influence on its transport activity (Fig. 2A). The negative control, consisting of membrane vesicles from eYFP-overexpressing HEK293 cells, showed no expression of MRP1-4.

Concentration-dependent transport of $E_2$17βG into MRP1, MRP2, MRP3, and MRP4 overexpressing membrane vesicles

Concentration-dependent uptake of $E_2$17βG into membrane vesicles was measured after 5 minutes for all transporters and typical curves are shown in Figure 2A-D. ATP-dependent $E_2$17βG transport reached maximum activities (V_{max}) of 31 ± 1, 2220 ± 100, and 94 ± 5 pmol mg^{-1} min^{-1} for MRP1, MRP3, and MRP4, respectively. The affinity of $E_2$17βG (K_m) for MRP1, MRP3, and MRP4 was 7.5 ± 0.1 µM, 56 ± 6 µM, and 15 ± 3 µM, respectively. Repetition of the experiment for each transporter gave comparable kinetic parameters, only the V_{max} of MRP3 varied between different batches of membrane vesicles, due to different expression levels of the transporter. Transport activity of MRP2 followed a sigmoidal relationship with increased $E_2$17βG concentration (Fig. 2B). A Hill slope of 1.6 ± 0.03 was calculated for MRP2 activity, which is indicative of positive cooperativity.

Effects of 3,4-diarylpyrazolines and rimonabant on MRP1-, MRP2-, MRP3-, and MRP4-mediated $E_2$17βG transport

Based on the kinetics of $E_2$17βG uptake by MRP1-4, the following $E_2$17βG concentrations, well below the K_m, were chosen for interaction studies with 3,4-diarylpyrazolines and rimonabant (Fig. 1): 0.16 µM for MRP1, 20 µM for MRP2, 0.08 µM for MRP3, and 0.12 µM for MRP4. In the case of MRP2, 20 µM substrate was used to measure both stimulation and inhibition.

Figure 3 shows the effect of 10 and 100 µM of the CB1 receptor antagonists on $E_2$17βG transport by MRP1-4. Due to poor solubility, the actual concentrations of the 3,4-diarylpyrazolines

DMD Fast Forward. Published on April 21, 2011 as DOI: 10.1124/dmd.110.037812
This article has not been copyedited and formatted. The final version may differ from this version.

and rimonabant were 3- to 100-fold lower than the predicted concentrations (see legend of Fig. 3). The highest concentration of the series of 3,4-diarylpyrazolines inhibited MRP4 transport activity (Fig. 3D) more potently than MRP1 (Fig. 3A). Of the 3,4-diarylpyrazolines, compounds 4, and 12-14 significantly inhibited MRP1- and MRP4-mediated $E_2$17βG transport. Compound 13 had the highest inhibitory effect on both transporters, with -34 ± 13% and -72 ± 8% for MRP1 and MRP4, respectively. Transport of $E_2$17βG by MRP1 and MRP4 was not inhibited by compounds 15-17, and 23, whereas compound 11 did inhibit MRP4, but not MRP1. Rimonabant inhibited MRP1 more potently than MRP4, *viz.* -84 ± 4% versus -58 ± 3% (Fig. 3A and 4D). In contrast to MRP1 and MRP4, MRP2 transport activity was stimulated by most compounds, at both concentrations tested (Fig. 3B). At the lower concentration, compounds 15-17 significantly increased uptake of $E_2$17βG into MRP2 vesicles (256-305%). Stimulation of MRP2 was strongest at the high concentration of compounds 4-14 (543-734%) and less by 15-17 (349-412%) and rimonabant (513%). Compound 23 did not significantly increase transport. Figure 3C shows that, although $E_2$17βG itself inhibited transport, MRP3-mediated $E_2$17βG transport was significantly stimulated by rimonabant and most 3,4-diarylpyrazolines, of which 11 and 13 had the highest stimulatory effect (~155%).

Mechanism of modulation of MRP1-4 transport by compounds 13, 15, and rimonabant

To get a better understanding of the mechanism of interaction, we measured concentration-dependent effects of certain CB1 receptor antagonists on MRP1-4 transport at three different $E_2$17βG concentrations for each transporter (Fig. 4). 3,4-Diarylpyrazoline derivatives 13 and 15, and rimonabant were selected for further investigation because the magnitude of their effects on the transport activity were different.

Increasing $E_2$17βG concentrations did not decrease the potency of 3,4-diarylpyrazolines 13 and 15, and rimonabant for inhibiting MRP1 and MRP4 (Fig. 4A-C and 4J-L); the percentage of inhibition and the IC_{50} values of 13 and rimonabant for MRP4 and MRP1 were similar at different $E_2$17βG concentrations. Dixon plots for 13- and rimonabant-mediated inhibition of MRP4 and MRP1 show that the lines intersected virtually at the *x*-axis for both compounds, which is indicative of non-competitive inhibition (Fig. 5A-C). The intersections corresponded to a K_i of ~ 1.4 μM of rimonabant

DMD Fast Forward. Published on April 21, 2011 as DOI: 10.1124/dmd.110.037812
This article has not been copyedited and formatted. The final version may differ from this version.

for MRP1, ~ 4 µM of rimonabant for MRP4, and ~ 7 µM of 13 for MRP4. 3,4-Diarylpyrazoline 15 did not inhibit MRP1 transport activity at any of the concentrations tested and only moderately inhibited MRP4 (Fig. 4A-C and 4J-L).

MRP2-mediated transport was stimulated by compounds 13, 15, and rimonabant at the lowest $E_2$17βG concentration of 2 µM (Fig. 4D). Stimulation was decreased at 20 µM $E_2$17βG, and transport was inhibited at 200 µM of $E_2$17βG (Fig. 4D-F). Rimonabant and compound 15 appeared to have the same stimulatory and inhibitory potency on MRP2-mediated transport.

MRP3-mediated $E_2$17βG transport was stimulated at low substrate concentration, which gradually disappeared at higher substrate concentrations (Fig. 4G-I). At a concentration of 15 µM $E_2$17βG, high concentrations of compounds 13, 15, and rimonabant inhibited $E_2$17βG transport via MRP3 (data not shown).

In vivo pharmacodynamic effect of 3,4-diarylpyrazolines on CP55,940 induced hypotension in rat

To get an impression of the relative brain penetration of the 3,4-diarylpyrazolines, the CB1 receptor-mediated blood pressure effect of compounds 4, 11, 14, and 15 was compared with their *in vitro* CB1 receptor binding affinity. For this purpose, in rats, the initial rapid effect was measured of CB1 receptor antagonists on CP55,940-induced hypotension, which is considered to originate primarily from a central sympathetic response (Vollmer et al., 1974). Table 2 describes the effective intravenous dose (ED_{50}) that was needed for 50% inhibition of the hypotensive effect of CP55,940, and the binding affinity (expressed as K_i) of these compounds for the CB1 receptor, as determined previously (Lange et al., 2005). The *in vivo* data show that CB1 receptor antagonist 15 had the lowest ED_{50} value. If the ED_{50} of 15 relative to its binding affinity is extrapolated to compounds 4, 11, and 14 on basis of their K_i values for the CB1 receptor, ED_{50} values of 0.14, 0.02 , and 0.15 mg/kg, respectively, would have been expected. However, the actual ED_{50} values of compounds 4, 11, and 14 (Table 2) were >2, ~10, and ~4.7 times higher than expected, indicating a lower brain permeability compared to compound 15.

DMD Fast Forward. Published on April 21, 2011 as DOI: 10.1124/dmd.110.037812
This article has not been copyedited and formatted. The final version may differ from this version.

Discussion

This study shows that CB1 receptor antagonists interacted with the efflux transporters MRP1, MRP2, MRP3, and MRP4. $E_2$17βG was used as a model substrate to investigate the effect of CB1 receptor antagonists on transport activity of these transporters. The kinetic parameters for $E_2$17βG found in this study were comparable with literature (Loe et al., 1996;Zeng et al., 2000;Chen et al., 2001). Unlike MRP1, MRP3, and MRP4, MRP2 transported $E_2$17βG in a positive cooperative manner, which was previously demonstrated by others (Zelcer et al., 2003;Bodó et al., 2003a).

Actual tested concentrations of the very lipophilic CB1 receptor antagonists in the experimental assays were determined by LC-MS/MS and were 3- to 100-fold lower than expected. This may be due to incomplete dissolution or non-specific binding. In our study, compounds 15-17 stimulated MRP2 better than compounds 4-14 at low concentrations. In contrast, the opposite was found at higher concentrations, where the actual concentrations of compounds 15-17 were lower (1-3 μM) than those of 4-14 (7-33 μM) (Fig. 3). This indicates that compounds 15-17, which contain N-substituents that make them more lipophilic, have a higher potency in affecting MRP2 but have a limited effect due to their low solubility. The same was found for MRP3, and the lack of effect of compounds 15-23 on MRP1 and MRP4 might also be explained by their low actual concentrations.

Although we used $E_2$17βG as a substrate for all transporters, the effect of the CB1 receptor antagonists on transport of this substrate via MRP1-4 was different. MRP1- and MRP4-mediated transport was inhibited by several CB1 receptor antagonists. The inhibitory affinity of rimonabant was somewhat higher for MRP1-mediated $E_2$17βG transport than for MRP4-mediated transport, with a K_i of ~1.4 μM versus ~ 4 μM. The maximum plasma concentration found in male human subjects treated with a therapeutic dose of rimonabant is 0.4 μM (Turpault et al., 2006). Rimonabant and 3,4-diarylpyrazoline 13 appeared to inhibit MRP1 and MRP4 in a non-competitive manner (Fig. 5A-C). In addition, MRP1 and MRP4 were stimulated at low substrate and rimonabant concentrations, indicating that rimonabant probably does not compete for the $E_2$17βG binding site of both transporters (Fig. 4A and 4J). Whether rimonabant and the 3,4-diarylpyrazolines are only inhibitors or also substrates of MRP1 or MRP4 cannot be concluded from this study.

DMD Fast Forward. Published on April 21, 2011 as DOI: 10.1124/dmd.110.037812
This article has not been copyedited and formatted. The final version may differ from this version.

In contrast to MRP1 and MRP4, MRP2-mediated transport was stimulated by all CB1 receptor antagonists, except for compound 23. The results presented in this study suggest that 3,4-diarylpyrazolines and rimonabant stimulate MRP2 allosterically at low $E_2$17βG concentrations and compete for the $E_2$17βG binding site at high concentrations. This type of interaction is supported by other studies (Zelcer et al., 2003;Bakos et al., 2000;Evers et al., 2000). The study of Zelcer *et al.* (2003) showed that several aromatic compounds, most of them containing sulfoxide or tosyl groups, stimulate MRP2-mediated transport of $E_2$17βG into membrane vesicles. Compounds that normalized the stimulated transport rates at increasing concentrations, such as sulfinpyrazone and indomethacin, also appeared to be substrates for MRP2 (Zelcer et al., 2003;Evers et al., 2000). 3,4-Diarylpyrazolines chemically resemble sulfinpyrazone, which, together with the fact that compounds 13, 15, and rimonabant might compete with $E_2$17βG at higher substrate concentrations, could indicate that they are substrates for MRP2.

The CB1 receptor antagonists had comparable effects on MRP3 transport activity, but their effects were less pronounced than for MRP2 (Fig. 4G-I). Other studies reported that MRP3-mediated $E_2$17βG transport activity can be inhibited as well as stimulated by different compounds, *e.g.* E3040-sulfate, indomethacin, benzbromarone (Akita et al., 2002;Bodó et al., 2003a;Bodó et al., 2003b). This indicates that the 3,4-diarylpyrazolines and rimonabant would interact with a modulating site and the substrate site of MRP3, causing stimulation of $E_2$17βG transport at low substrate concentrations and inhibition at higher substrate concentrations due to competition for the substrate site.

Our results show that rimonabant and 3,4-diarylpyrazolines can modulate MRP1-4 transport activity, which implicates the possibility of drug-drug interactions. Because of the brief clinical use of rimonabant, few data are available on its *in vivo* interaction potential with drug transporters. Rimonabant was found to moderately affect the pharmacokinetics of the P-glycoprotein (P-gp/ABCB1) substrate cyclosporine A, but not of tacrolimus and digoxin (Amundsen et al., 2009;Kanamaluru et al., 2005).

The pharmacokinetic data available for rimonabant do not suggest an important role for the MRPs in determining its disposition. Rimonabant is shown to accumulate in fat tissue, spleen, thyroid, thymus, liver, plasma, and brain and reported to cross the placental barrier (Barna et al., 2009)(EMA -

EPAR Scientific discussion about rimonabant). Although rimonabant showed a strong interaction with MRP1, its accumulation in the brain and passage across the placental barrier indicates that it is either a poor substrate of this transporter, or MRP1 is not efficacious enough as a barrier for rimonabant.

MRP1 and MRP4 are expressed at the blood-brain-barrier and the choroid plexus, where these transporters could be involved in limiting the brain penetration of the 3,4-diarylpyrazoline CB1 receptor antagonists. Because there are only minor differences in the structures of the 3,4-diarylpyrazolines, the rate and extent of passive diffusion of these compounds into the brain and other tissues is expected to be similar, which should reflect in a similar relationship between ED_{50} and CB1 receptor binding affinity (K_i). However, there was a difference in ED_{50} values for compounds 4, 11, 14, and 15, which could not solely be attributed to differences in CB1 receptor binding affinities. The ED_{50} of compounds 4, 11, and 14 relative to their K_i values were higher as compared to the ED_{50}/K_i ratio of compound 15 (Table 2). This suggests that an active mechanism is lowering the concentration of compounds 4, 11 and 14 at the site of action, resulting in increased ED_{50} values. As the rapid hypotensive action of CB1 agonists was shown to be primarily dependent on centrally-mediated sympathetic tone (Vollmer et al., 1974), this could implicate that compounds 4, 11 and 14, but not 15, have a higher ED_{50} because they are less brain permeable. Our *in vitro* data suggest that MRP4 might be involved. To draw definite conclusions about the involvement of MRP1-4 in influencing tissue concentrations of 3,4-diarylpyrazolines, *in vivo* studies should be performed using specific transport inhibitors and/or *Mrp* knockout mice.

In addition, it will be important to measure direct transport of CB1 receptor antagonists by MRP1-4 *in vitro*. Isolated membrane vesicles are likely not useful for this purpose due to high nonspecific binding to lipid membranes and high passive diffusion of the lipophilic CB1 receptor antagonists (unpublished results). Cell-based accumulation or vectorial transport studies may be more suitable. Furthermore, the role of the blood-brain-barrier and intestinal ABC transporters P-gp and Breast Cancer Resistance Protein (BCRP/ABCG2) as possible CB1 receptor antagonist efflux pumps should be investigated. The role of influx transporters should also be considered in the tissue distribution of the CB1 receptor antagonists, but it is to be expected that uptake of these lipophilic compounds will be governed largely by passive diffusion.

In conclusion, we have shown that 3,4-diarylpyrazolines and rimonabant inhibited MRP1- and MRP4-mediated $E_2$17βG transport and stimulated MRP2- and MRP3-mediated transport at low $E_2$17βG concentrations. Stimulation of MRP2 and MRP3 shifted to inhibition at increasing substrate concentrations. The effect of these compounds on the transport activity of MRP1-4 shows the potential for possible drug-drug interactions. Preliminary *in vivo* data suggested that MRP4 could be involved in the lower brain permeability of some of the 3,4-diarylpyrazolines. The actual role of MRPs in tissue distribution of 3,4-diarylpyrazolines and rimonabant remains to be investigated. In addition, this study shows that the modulatory effects of the 3,4-diarylpyrazolines were influenced by the properties of their N-substituent, which indicates that small variations in their chemical structure can determine the affinity for the efflux transporters and thereby possibly affect their pharmacokinetic behavior.

Acknowledgements

We thank Abbott Healthcare Products B.V. (formerly Solvay Pharmaceuticals) for providing the in vivo pharmacology data (MJP Adolfs Ing.). We thank Dr. Kevin Weigl (Abbott Products GmbH) for his critical reading of the manuscript.

Authorship contributions

Participated in research design: Wittgen, Dinter-Heidorn, Koenderink, and Russel.

Conducted experiments: Wittgen and van den Heuvel.

Contributed new reagents or analytic tools: Dinter-Heidorn and van den Broek.

Performed data analysis: Wittgen and van den Heuvel.

Wrote or contributed to the writing of the manuscript: Wittgen, Koenderink, and Russel.

DMD Fast Forward. Published on April 21, 2011 as DOI: 10.1124/dmd.110.037812
This article has not been copyedited and formatted. The final version may differ from this version.

Reference List

Akita H, Suzuki H, Hirohashi T, Takikawa H and Sugiyama Y (2002) Transport Activity of Human MRP3 Expressed in Sf9 Cells: Comparative Studies With Rat MRP3. *Pharm Res* **19**:34-41.

Amundsen R, Asberg A, Robertsen I, Vethe N T, Bergan S, Hartmann A and Midtvedt K (2009) Rimonabant Affects Cyclosporine A, but Not Tacrolimus Pharmacokinetics in Renal Transplant Recipients. *Transplantation* **87**:1221-1224.

Bakos E, Evers R, Sinko E, Varadi A, Borst P and Sarkadi B (2000) Interactions of the Human Multidrug Resistance Proteins MRP1 and MRP2 With Organic Anions. *Mol Pharmacol* **57**:760-768.

Barna I, Till I and Haller J (2009) Blood, Adipose Tissue and Brain Levels of the Cannabinoid Ligands WIN-55,212 and SR-141716A After Their Intraperitoneal Injection in Mice: Compound-Specific and Area-Specific Distribution Within the Brain. *Eur Neuropsychopharmacol* **19**:533-541.

Bifulco M, Santoro A, Laezza C and Malfitano A M (2009) Cannabinoid Receptor CB1 Antagonists: State of the Art and Challenges. *Vitam Horm* **81**:159-189.

Bodó A, Bakos E, Szeri F, Váradi A and Sarkadi B (2003a) Differential Modulation of the Human Liver Conjugate Transporters MRP2 and MRP3 by Bile Acids and Organic Anions. *J Biol Chem* **278**:23529-23537.

Bodó A, Bakos E, Szeri F, Váradi A and Sarkadi B (2003b) The Role of Multidrug Transporters in Drug Availability, Metabolism and Toxicity. *Toxicol Lett* **140-141**:133-143.

Boyd ST and Fremming B A (2005) Rimonabant-a Selective CB1 Antagonist. *Ann Pharmacother* **39**:684-690.

Chen ZS, Lee K and Kruh G D (2001) Transport of Cyclic Nucleotides and Estradiol 17-Beta-D-Glucuronide by Multidrug Resistance Protein 4. Resistance to 6-Mercaptopurine and 6-Thioguanine. *J Biol Chem* **276**:33747-33754.

Conrad S, Kauffmann H M, Ito K, Deeley R G, Cole S P and Schrenk D (2001) Identification of Human Multidrug Resistance Protein 1 (MRP1) Mutations and Characterization of a G671V Substitution. *J Hum Genet* **46**:656-663.

Di Marzo V (2008) CB1 Receptor Antagonism: Biological Basis for Metabolic Effects. *Drug Discov Today* **13**:1026-1041.

El-Sheikh AA, van den Heuvel J J, Koenderink J B and Russel F G (2007) Interaction of Nonsteroidal Anti-Inflammatory Drugs With Multidrug Resistance Protein (MRP) 2/ABCC2- and MRP4/ABCC4-Mediated Methotrexate Transport. *J Pharmacol Exp Ther* **320**:229-235.

El-Sheikh AA, van den Heuvel J J, Krieger E, Russel F G and Koenderink J B (2008) Functional Role of Arginine 375 in Transmembrane Helix 6 of Multidrug Resistance Protein 4 (MRP4/ABCC4). *Mol Pharmacol* **74**:964-971.

Evers R, de H M, Sparidans R, Beijnen J, Wielinga P R, Lankelma J and Borst P (2000) Vinblastine and Sulfinpyrazone Export by the Multidrug Resistance Protein MRP2 Is Associated With Glutathione Export. *Br J Cancer* **83**:375-383.

Flens MJ, Zaman G J, van der Valk P, Izquierdo M A, Schroeijers A B, Scheffer G L, van der Groep P., de Haas M., Meijer C J and Scheper R J (1996) Tissue Distribution of the Multidrug Resistance Protein. *Am J Pathol* **148**:1237-1247.

Ito S, Ieiri I, Tanabe M, Suzuki A, Higuchi S and Otsubo K (2001) Polymorphism of the ABC Transporter Genes, MDR1, MRP1 and MRP2/CMOAT, in Healthy Japanese Subjects. *Pharmacogenetics* **11**:175-184.

Jones D (2008) End of the Line for Cannabinoid Receptor 1 As an Anti-Obesity Target? *Nat Rev Drug Discov* **7**:961-962.

Kanamaluru V, Lockwood G, Bonnet D and Newton J (2005) Lack of Effect of Rimonabant on the Pharmacokinetics of Digoxin. *Journal of Clinical Pharmacology* **45**:1081.

Kruh GD and Belinsky M G (2003) The MRP Family of Drug Efflux Pumps. *Oncogene* **22**:7537-7552.

Lange JH, Coolen H K, van Stuivenberg H H, Dijksman J A, Herremans A H, Ronken E, Keizer H G, Tipker K, McCreary A C, Veerman W, Wals H C, Stork B, Verveer P C, den Hartog A P, de Jong N M, Adolfs T J, Hoogendoorn J and Kruse C G (2004) Synthesis, Biological Properties, and Molecular Modeling Investigations of Novel 3,4-Diarylpyrazolines As Potent and Selective CB(1) Cannabinoid Receptor Antagonists. *J Med Chem* **47**:627-643.

Lange JH, van Stuivenberg H H, Veerman W, Wals H C, Stork B, Coolen H K, McCreary A C, Adolfs T J and Kruse C G (2005) Novel 3,4-Diarylpyrazolines As Potent Cannabinoid CB1 Receptor Antagonists With Lower Lipophilicity. *Bioorg Med Chem Lett* **15**:4794-4798.

Leslie EM, Deeley R G and Cole S P (2005) Multidrug Resistance Proteins: Role of P-Glycoprotein, MRP1, MRP2, and BCRP (ABCG2) in Tissue Defense. *Toxicol Appl Pharmacol* **204**:216-237.

Loe DW, Almquist K C, Cole S P and Deeley R G (1996) ATP-Dependent 17ß-Estradiol 17-(ß-D-Glucuronide) Transport by Multidrug Resistance Protein (MRP). Inhibition by Cholestatic Steroids. *J Biol Chem* **271**:9683-9689.

Nies AT, Jedlitschky G, Konig J, Herold-Mende C, Steiner H H, Schmitt H P and Keppler D (2004) Expression and Immunolocalization of the Multidrug Resistance Proteins, MRP1-MRP6 (ABCC1-ABCC6), in Human Brain. *Neuroscience* **129**:349-360.

Nies AT and Keppler D (2007) The Apical Conjugate Efflux Pump ABCC2 (MRP2). *Pflugers Arch* **453**:643-659.

Nissen SE, Nicholls S J, Wolski K, Rodés-Cabau J, Cannon C P, Deanfield J E, Després J P, Kastelein J J, Steinhubl S R, Kapadia S, Yasin M, Ruzyllo W, Gaudin C, Job B, Hu B, Bhatt D L, Lincoff A M and Tuzcu E M (2008) Effect of Rimonabant on Progression of Atherosclerosis in Patients With Abdominal Obesity and Coronary Artery Disease: the STRADIVARIUS Randomized Controlled Trial. *JAMA* **299**:1547-1560.

Rao VV, Dahlheimer J L, Bardgett M E, Snyder A Z, Finch R A, Sartorelli A C and Piwnica-Worms D (1999) Choroid Plexus Epithelial Expression of MDR1 P Glycoprotein and Multidrug Resistance-Associated Protein Contribute to the Blood-Cerebrospinal-Fluid Drug-Permeability Barrier. *Proc Natl Acad Sci U S A* **96**:3900-3905.

Russel FGM, Koenderink J B and Masereeuw R (2008) Multidrug Resistance Protein 4 (MRP4/ABCC4): a Versatile Efflux Transporter for Drugs and Signalling Molecules. *Trends Pharmacol Sci* **29**:200-207.

Scheffer GL, Kool M, de Haas M., de Vree J M, Pijnenborg A C, Bosman D K, Oude Elferink R P, van der Valk P, Borst P and Scheper R J (2002) Tissue Distribution and Induction of Human Multidrug Resistant Protein 3. *Lab Invest* **82**:193-201.

Smeets PH, van Aubel R A, Wouterse A C, van den Heuvel J J and Russel F G (2004) Contribution of Multidrug Resistance Protein 2 (MRP2/ABCC2) to the Renal Excretion of P-Aminohippurate (PAH) and Identification of MRP4 (ABCC4) As a Novel PAH Transporter. *J Am Soc Nephrol* **15**:2828-2835.

Tam J, Vemuri V K, Liu J, Batkai S, Mukhopadhyay B, Godlewski G, Osei-Hyiaman D, Ohnuma S, Ambudkar S V, Pickel J, Makriyannis A and Kunos G (2010) Peripheral CB1 Cannabinoid Receptor Blockade Improves Cardiometabolic Risk in Mouse Models of Obesity. *J Clin Invest* **120**:2953-2966.

Turpault S, Kanamaluru V, Lockwood G F, Bonnet D and Newton J (2006) Rimonabant Pharmacokinetics in Healthy and Obese Subjects. *Clinical Pharmacology & Therapeutics* **79**:50.

van Aubel RA, Hartog A, Bindels R J, Van Os C H and Russel F G (2000) Expression and Immunolocalization of Multidrug Resistance Protein 2 in Rabbit Small Intestine. *Eur J Pharmacol* **400**:195-198.

van Aubel RA, Koenderink J B, Peters J G, Van Os C H and Russel F G (1999) Mechanisms and Interaction of Vinblastine and Reduced Glutathione Transport in Membrane Vesicles by the Rabbit Multidrug Resistance Protein Mrp2 Expressed in Insect Cells. *Mol Pharmacol* **56**:714-719.

van Aubel RA, Smeets P H, Peters J G, Bindels R J and Russel F G (2002) The MRP4/ABCC4 Gene Encodes a Novel Apical Organic Anion Transporter in Human Kidney Proximal Tubules: Putative Efflux Pump for Urinary CAMP and CGMP. *J Am Soc Nephrol* **13**:595-603.

Vollmer RR, Cavero I, Ertel R J, Solomon T A and Buckley J P (1974) Role of the Central Autonomic Nervous System in the Hypotension and Bradycardia Induced by (-)-Delta 9-Trans-Tetrahydrocannabinol. *J Pharm Pharmacol* **26**:186-192.

Yu XQ, Xue C C, Wang G and Zhou S F (2007) Multidrug Resistance Associated Proteins As Determining Factors of Pharmacokinetics and Pharmacodynamics of Drugs. *Curr Drug Metab* **8**:787-802.

Zelcer N, Huisman M T, Reid G, Wielinga P, Breedveld P, Kuil A, Knipscheer P, Schellens J H, Schinkel A H and Borst P (2003) Evidence for Two Interacting Ligand Binding Sites in Human Multidrug Resistance Protein 2 (ATP Binding Cassette C2). *J Biol Chem* **278**:23538-23544.

Zeng H, Liu G, Rea P A and Kruh G D (2000) Transport of Amphipathic Anions by Human Multidrug Resistance Protein 3. *Cancer Res* **60**:4779-4784.

Zhou SF, Wang L L, Di Y M, Xue C C, Duan W, Li C G and Li Y (2008) Substrates and Inhibitors of Human Multidrug Resistance Associated Proteins and the Implications in Drug Development. *Curr Med Chem* **15**:1981-2039.

Footnotes

This work was funded by the Dutch Top Institute Pharma and was performed within the framework of project T5-105.

Prof. F.G.M. Russel, PhD, Department of Pharmacology and Toxicology (149), Radboud University Nijmegen Medical Centre, Nijmegen Centre for Molecular Life Sciences, P. O. Box 9101, 6500 HB Nijmegen, the Netherlands. E-mail: F.Russel@pharmtox.umcn.nl

DMD Fast Forward. Published on April 21, 2011 as DOI: 10.1124/dmd.110.037812
This article has not been copyedited and formatted. The final version may differ from this version.

Legends

Fig. 1. Chemical structure of CB1 receptor antagonists. Core structure of 3,4-diarylpyrazolines derivatives 4, 11-17, and 23 (A) with the chemical structures of **R** for the N-substituent of these compounds (B) (Lange et al., 2005). Structure of rimonabant (C).

Fig. 2. Kinetics of ATP-dependent $E_2$17βG transport into membrane vesicles of HEK293 cells overexpressing MRP1 (A), MRP2 (B), MRP3 (C), or MRP4 (D). Concentration-dependent $E_2$17βG transport was determined after 5 minutes for all transporters. ATP-dependent eYFP values were subtracted from corresponding ATP-dependent MRP values and K_m and V_{max} were determined by non-linear regression analysis (D-F). Data points represent the mean ± S.E.M of triplicate measurements in a representative experiment.

Fig. 3. Effect of CB1 receptor antagonists on ATP-dependent transport of $E_2$17βG into MRP1- (A), MRP2- (B), MRP3- (C), or MRP4-overexpressing membrane vesicles (D). Transport was measured during five minutes at concentrations of 0.16, 20, 0.08, and 0.12 µM $E_2$17βG, for MRP1, MRP2, MRP3, and MRP4, respectively, in the absence (white bars) or presence of CB1 receptor antagonists. Due to their poor solubility, concentrations in the low range varied between 0.4 and 2.2 µM (grey bars) and between 4 and 33 µM (black bars) for the 10-fold higher range. Actual concentrations of CB1 receptor antagonists corresponding to the grey bars were 2.2 µM for compound 4, 0.7-1.3 µM for 11-23, and 0.4 µM for rimonabant. Actual concentrations corresponding to the black bars were 33 µM for CB1 receptor antagonist 4, 7 µM for 11-12, 12 µM for 13-14, 1-3 µM for 15-23, and 4 µM for rimonabant. ATP-dependent uptake in absence of CB1 receptor antagonists was set at 100% (white bar) and was also measured in presence of 100 µM $E_2$17βG (black bar). Mean ± S.E.M of three independent experiments is shown. Statistically significant differences from vehicle control: * $p < 0.05$, ** $p < 0.01$, and *** $p < 0.001$.

Fig. 4. Effect of CB1 receptor antagonists 13 (◊), 15 (▲, dotted line), and rimonabant (●) on MRP-mediated $E_2$17βG transport at different substrate concentrations. $E_2$17βG concentrations were 0.16

DMD Fast Forward. Published on April 21, 2011 as DOI: 10.1124/dmd.110.037812
This article has not been copyedited and formatted. The final version may differ from this version.

(A), 1 (B), and 5 µM (C) for MRP1. For MRP2, these were 2 (D), 20 (E), and 200 µM (F), for MRP3 0.08 (G), 1 (H), and 5 µM (I), and for MRP4 0.1 (J), 0.3 (K), and 1 µM (L). ATP-dependent transport was determined after five minutes for MRP1, MRP2, and MRP4, and after 2 minutes for MRP3. Transport rates were expressed as a percentage of uptake measured in the absence of the CB1 receptor antagonist tested against the log drug concentration. Two to three independent experiments were performed in duplicate. Mean ± S.E.M of n = 3-6 is shown.

Fig. 5. Dixon plots of inhibition of MRP1- and MRP4-mediated ATP-dependent $E_2$17βG transport by rimonabant and 3,4-diarylpyrazoline 13. The reciprocal of transport velocity (1/V) of different substrate concentrations is plotted against the inhibitor concentration. Dixon plots of inhibition of MRP1 (A) and MRP4 (B) by rimonabant, and of MRP4 by 13 (C) at three different $E_2$17βG concentrations are shown (● 0.16 µM, ◊ 1 µM, and ▲ 5 µM for $E_2$17βG MRP1, and for MRP4, ■ 0.1 µM, Δ 0.3 µM, and ♦ 1 µM $E_2$17βG). Linear regression analysis was used for plotting lines and determination of K_i. Data represent the mean 1/V of duplicate measurements in a representative experiment.

DMD Fast Forward. Published on April 21, 2011 as DOI: 10.1124/dmd.110.037812
This article has not been copyedited and formatted. The final version may differ from this version.

Table 1. LC-MS/MS conditions for detection of CB1 receptor antagonists

Compound	Retention time (min)	Parent (*m/z*)	Product 1 (CE) (*m/z*) (eV)	Product 2 (CE) (*m/z*) (eV)	S-lens (V)
4	3.2	420.182	255.060 (27)	375.140 (13)	115
11	4.2	448.222	255.100 (26)	375.080 (16)	108
12	4.2	448.221	255.060 (30)	375.050 (14)	111
13	3.8	434.204	255.060 (26)	375.090 (14)	109
14	3.5	446.205	255.090 (28)	375.100 (16)	118
15	4.8	474.245	255.070 (29)	375.100 (28)	127
16	5.4	488.261	255.060 (31)	375.090 (19)	130
17	4.0	478.184	255.050 (28)	375.000 (15)	113
23	2.6	510.169	255.080 (29)	375.100 (15)	127
rimonabant	3.2	463.163	299.000 (46)	363.020 (29)	125

CE: collision energy

DMD Fast Forward. Published on April 21, 2011 as DOI: 10.1124/dmd.110.037812
This article has not been copyedited and formatted. The final version may differ from this version.

Table 2. Pharmacodynamic characteristics of the CB1 receptor antagonists

Compound	CB1 $_{rb}$ [a] K_i (nM)	ED_{50} (mg/kg, *i.v.*) [b]
4	223 ± 103	> 0.3
11	30 ± 14	0.2
14	231 ± 66	0.7
15	155 ± 69	0.1

[a] CB1 $_{rb}$, displacement of specific CP55,940 binding in CHO cells stably transfected with human CB1 receptor, expressed as K_i ± SEM (nM), adapted from Lange *et al.* (Lange et al., 2005).

[b] Dose of CB1 receptor antagonist that attenuates CP55,940 induced hypotension in rats (n=2 per dose) with 50%.

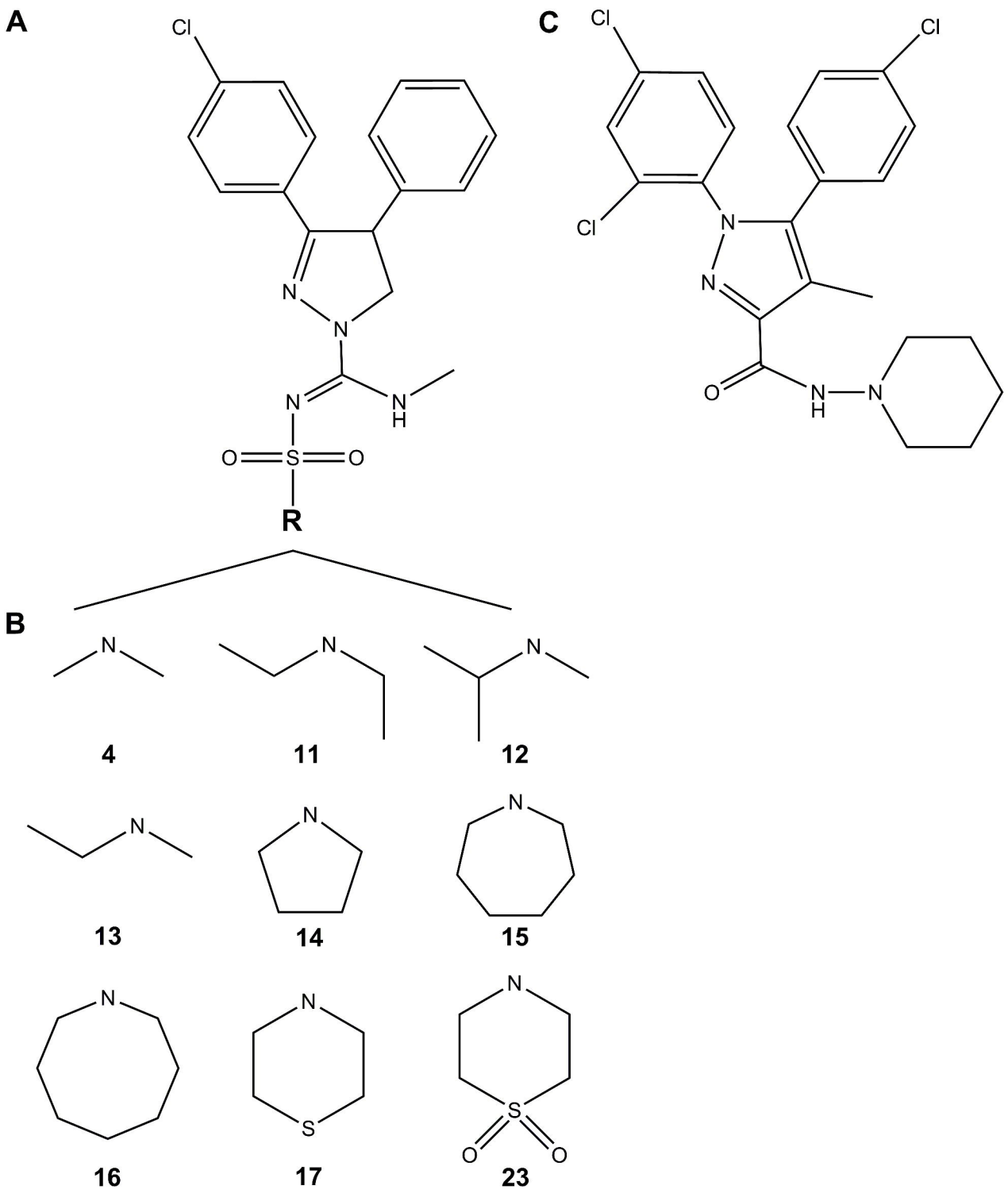
A
Cl
N
N
N
N
H
O
S
O
R
C
Cl
Cl
Cl
N
N
O
N
H
N
B
N
4
N
11
N
12
N
13
N
14
N
15
N
16
N
S
17
N
S
O
O
23

Figure 1

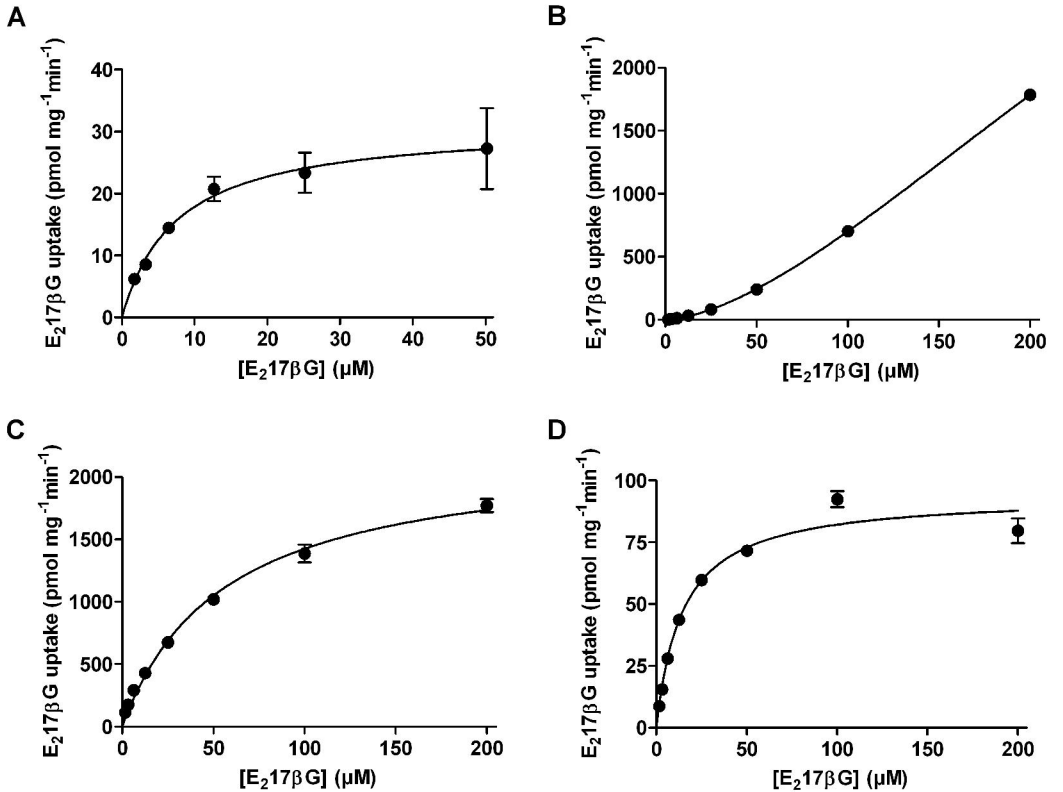
A
B
C
D
$E_2$17βG uptake (pmol mg^{-1}min^{-1})
[$E_2$17βG] (μM)
0
10
20
30
40
50
500
1000
1500
2000
25
75
100
150
200

Figure 2

Figure 3

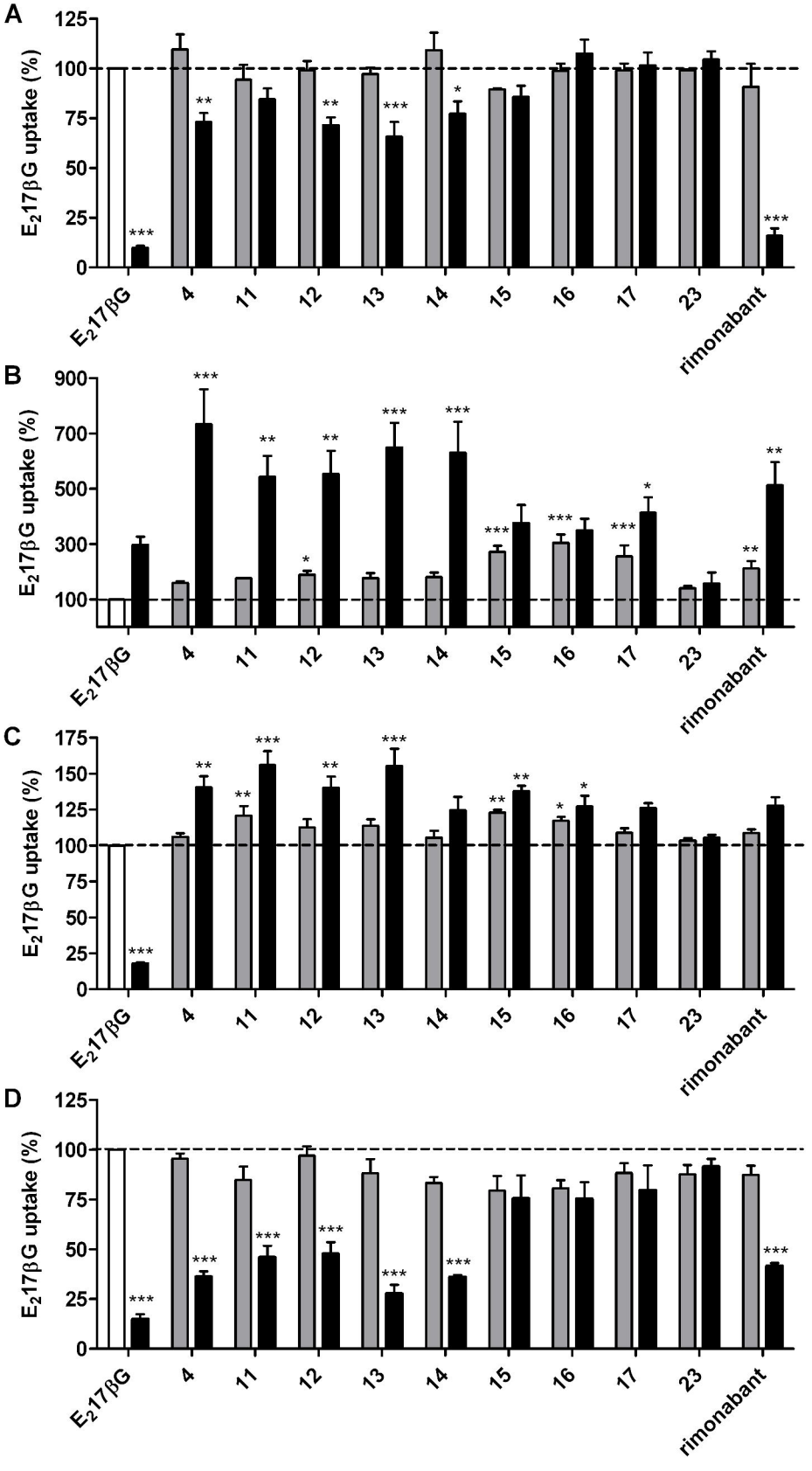

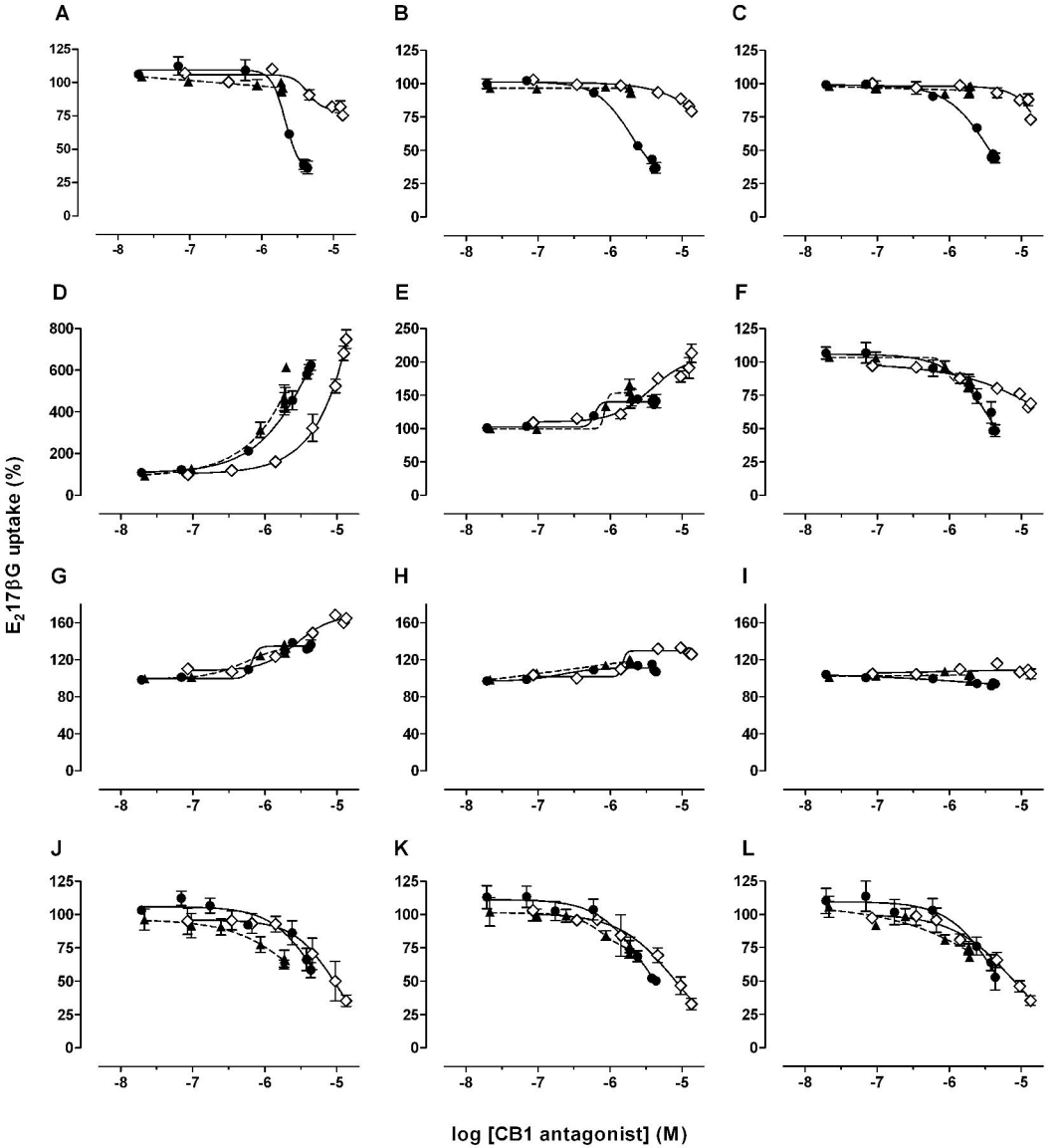

Figure 4

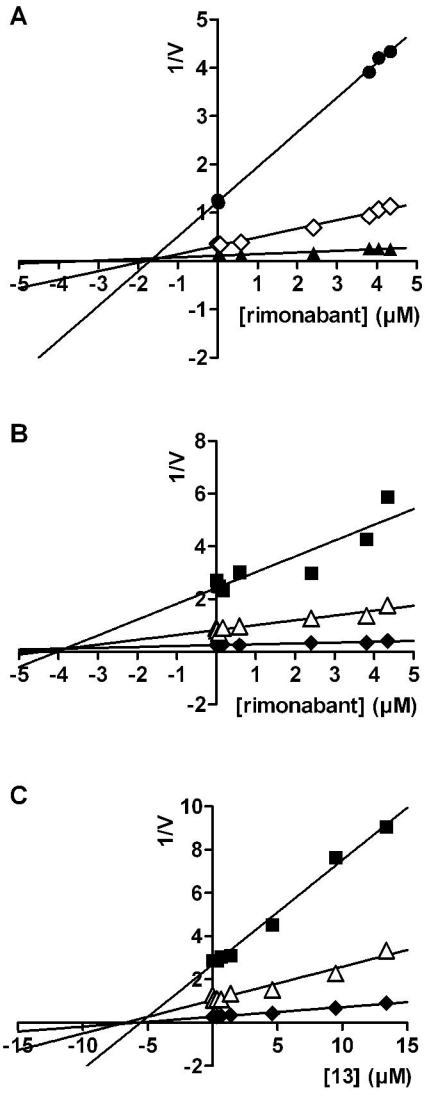
A
1/V
5
4
3
2
1
-1
-2
-5 -4 -3 -2 -1 1 2 3 4 5
[rimonabant] (μM)
B
1/V
8
6
4
2
-2
-5 -4 -3 -2 -1 1 2 3 4 5
[rimonabant] (μM)
C
1/V
10
8
6
4
2
-2
-15 -10 -5 5 10 15
[13] (μM)

Figure 5